VESSEL EXTRACTION USING ANISOTROPIC MINIMAL PATHS AND PATH SCORE

Da Chen, Laurent D. Cohen and Jean-Marie Mirebeau

CEREMADE, UMR 7534, Université Paris Dauphine PSL*, 75775 Paris Cedex 16, France

ABSTRACT

Geodesic methods have been widely applied to image analysis [1]. They are particularly efficient to extract a tubular structure, such as a blood vessel, given its two endpoints in a 2D or 3D medical image [2]. We address here a more difficult problem: the extraction of a full vessel tree structure given a single initial root, by growing a collection of keypoints, connected by geodesic minimal paths as in [3]. Keypoints are iteratively added, using selection criteria which compare *geodesic distances* with the standard *euclidean curve length* and a *path score*. A weakness of existing approaches is that the geodesic length and the euclidean path length are locally proportional, due to the use of an isotropic geodesic potential $\mathcal{P}(x)$. In contrast, we use an anisotropic geodesic potential $\mathcal{P}(x, v)$, and develop new criteria for selecting keypoints and stopping the tree growth. Experimental results demonstrate that our method can extract vessel structures at a finer scale, with increased accuracy.

***Index Terms*—** Vessel extraction, Anisotropic Fast Marching, Minimal Paths, Keypoints, Geodesic methods.

1. INTRODUCTION

Our work relies on the Cohen-Kimmel model [4], in which image features - vessel tubular structures, or object boundaries - are extracted under the form of minimal paths with respect to a geodesic energy potential $\mathcal{P}$. The geodesic potential can be isotropic [3], or anisotropic in the sense that path length depends on the path orientation [2]. It can be defined on the physical space, or involve additional abstract variables such as the extracted vessel radius [5]. Once this potential is properly defined, Fast Marching methods [6, 7, 8, 9] are the favored methods to estimate geodesic distances [4], from which minimal paths can be extracted. Paths on the image features are characterized by their small geodesic energy / euclidean length ratio. This selection criterion is combined with a path score in our vessel structure extraction algorithm. In order to make clear the specificity of our algorithm, which involves anisotropic potentials, and new keypoint selection and stopping criteria, we need to introduce some notations.

We introduce a mathematical domain $\Omega \subset \mathbb{R}^m$, connected open and bounded. As a first intuition, and as in the classical Cohen-Kimmel approach [4], Ω can be regarded as the physical image space. More recent and accurate feature extraction methods, pioneered by [5] and including this work, however define Ω as the product of physical space U with a parameter space $]r, R[$ representing vessel radius; vessel location and size are thus extracted and estimated in a single unified step. We denote by $\Im$ the collection of Lipschitz paths $\gamma : [0, 1] \to \overline{\Omega}$, and measure their length through a geodesic energy potential $\mathcal{P}(x, v)$:

$$l_{\mathcal{P}}(\gamma) := \int_0^1 \mathcal{P}(\gamma(t), \gamma'(t))dt. \tag{1}$$

The geodesic distance $\mathcal{U}(x)$, or minimal action map (MAM), is the minimal energy of any path joining a point $x \in \Omega$ to a given set of keypoints $\mathcal{K} \subset \Omega$:

$$\mathcal{U}(x) := \min\{l_{\mathcal{P}}(\gamma);\, \gamma \in \Im,\, \gamma(1) = x,\, \gamma(0) \in \mathcal{K}\}. \tag{2}$$

There always exists at least one minimal geodesic path γ_x, and only a single one for most x. Keypoints $\mathcal{K}$ represent in our application the currently extracted nodes of the vessel tree; should x be selected as a new keypoint, the path γ_x would be the connecting tree branch.

The classical Cohen-Kimmel model [4] relies on geodesic potentials of the form $\mathcal{P}(x, v) = (\mathcal{P}_0(x) + \omega)\|v\|$, where $\mathcal{P}_0$ is a Potential taking lower values around the interesting features of the images, and the positive constant w controls the smoothness of the minimal curve γ_x. Li and Yezzi [5] use potentials of the same form, but with the above mentioned additional radius dimension. Both the models [4] and [5] require user input endpoints as the prior knowledge to track the minimal paths. In order to reduce the user input, Benmansour and Cohen [3] proposed a new approach: keypoints searching method (KPSM) to detect recursively new startpoints (keypoints) along the expected features named, see §3. Kaul et al. [10] proposed a new stopping criteria for both open and closed curve detection and a new method to compute the curve length different to [3, 11]. Li et al. [12] proposed to detect the tubular structure using the extra radii model [5] and KPSM [3]. Benmansour and Cohen [2] enriched these constructions through the use of an anisotropic geodesic potential $\mathcal{P}(x, v) := \sqrt{v^T \mathcal{M}(x) v}$, where $\mathcal{M}$ is a tensor field of symmetric positive definite matrices, accounting for the orientation of the tubular structure.

In this paper we propose a new vessel tree extraction method based on automatic keypoints detection and state of the art Anisotropic FM [8]. The pairwise distances between keypoints are fixed by the curve length threshold (CLT); classical methods [3] tend to overlook parts of the vessel tree when the CLT is small, and to "leak" or take shortcuts between distinct branches or the vessel tree for large CLT (for details see section 4.1 and Figure 2). We substantially improve the performance for small CLT, by incorporating in the keypoint selection criterion a *Path Score*[13] computed from the optimally oriented flux centreline map (OOFCM) for each keypoint candidate detected by the classical definition. Summarily, Our contribution is as follows: 1) we redefine the keypoints to make them reasonable even for small curve length threshold. 2) We present the extension of the curve length calculation in the anisotropic case, in itself a different contribution. 3) We give a stopping criterion to automatically stop the keypoints searching scheme.

Convention: if Λ denotes a point (curve) with extra radii dimension, then we use $\widetilde{\Lambda}$ to denote a point (curve) with the same space location but without extra radii dimension, i.e. if $\Lambda = (x_0, y_0, r_0)$, then $\widetilde{\Lambda} = (x_0, y_0)$.

2. BACKGROUND

Our algorithm combines three main ingredients: construction of an anisotropic Riemannian metric, state of the art anisotropic fast marching with integrated geodesic curve length computation, and vessel tree extraction based on original and new selection criteria.

2.1. Optimally Oriented Flux and Metric construction

The oriented flux [14] of an image I, of dimension d, is defined by the amount of the image gradient projected along the orientation $\overrightarrow{\mathbf{p}}$ flowing out from a 2D circle (or 3D local sphere) at point $\widetilde{\mathbf{x}}$ with radius r:

$$f(\widetilde{x}; r, \overrightarrow{\mathbf{p}}) = \int_{\partial S_r} (\nabla(G_\sigma * I)(\widetilde{x} + r\overrightarrow{\mathbf{n}}) \cdot \overrightarrow{\mathbf{p}})(\overrightarrow{\mathbf{p}} \cdot \overrightarrow{\mathbf{n}}) dA, \quad (3)$$

where G_σ is a Gaussian function with variance σ and $\overrightarrow{\mathbf{n}}$ is the outward unit normal vector along ∂S_r. dA is the infinitesimal length (area) on ∂S_r. The oriented flux is a quadratic function: one has $f(\widetilde{x}; r, \overrightarrow{\mathbf{p}}) = \overrightarrow{\mathbf{p}}^T \cdot A(\widetilde{x}, r) \cdot \overrightarrow{\mathbf{p}}$ for some symmetric matrix $A(\widetilde{x}, r)$, which eigenvalues and eigenvectors we denote by $\lambda_i(\widetilde{x}, r)$ and $\mathbf{v}_i(\widetilde{x}, r)$. Law et al. [14] used the normalized sum of the non-zero eigenvalues to compute the OOFCM, which takes its largest values for points $\widetilde{x}$ in vessel centrelines (suppose that inside a vessel having stronger intensity than the background):

$$\hbar(\widetilde{x}) = \max_r \left\{ \frac{-1}{r^{d-1}} \sum_{i=1}^{d-1} \lambda_i(\widetilde{x}, r) \right\} \quad (4)$$

In this paper, use the same metric tensor as in [2]: the metric with additional radii dimension for the vessel extraction is as follows:

$$\mathcal{M}(\widetilde{\mathbf{x}}, r) = \begin{pmatrix} \mathcal{M}_s & \mathbf{0} \\ \mathbf{0} & \mathcal{M}_r \end{pmatrix}, \quad (5)$$

where $\mathcal{M}_s = \sum_{i=1}^d \exp(\alpha \sum_{j \neq i} \lambda_j) \mathbf{v}_i \mathbf{v}_i^T$ and $\mathcal{M}_r = \beta \exp(\sum_{i=1}^d \alpha \lambda_i)$, with implicit dependence on $(\widetilde{\mathbf{x}}, r)$. The constant β controls FM propagation speed along the radius direction, and α controls the metric anisotropy.

2.2. Anisotropic Fast Marching using Basis Reduction

Numerical methods for the minimal action map $\mathcal{U}(x)$, see (2), introduce a discretization grid Z of Ω, and for each $x \in Z$ a small mesh $S(x)$ of a neighborhood of x with vertices in Z (with the adequate modification if x is at or near the boundary). An approximation of $\mathcal{U}$ is given by the solution of the following fixed point problem: find $U : Z \to \mathbb{R}$ such that (i) $U(x) = 0$ for all keypoints $x \in \mathcal{K}$, and (ii) for all $x \in Z \setminus \mathcal{K}$

$$U(x) = \min_{y \in \partial S(x)} \mathcal{P}(x, y - x) + \mathrm{I}_{S(x)} U(y), \quad (6)$$

where I_S denotes piecewise linear interpolation on a mesh S. The expression (6) reflects the fact that the minimal path γ_x, joining x to $\mathcal{K}$, needs to cross the stencil boundary $\partial S(x)$ at some point y; hence it is the concatenation of a small path joining x to y, of approximate length $\mathcal{P}(x, y - x)$, and of γ_y, which energy is approximated by interpolation. A striking fact is that this N-dimensional fixed point system, with $N = \#(Z)$, can be solved in a single pass using the Fast Marching algorithm [6], provided the stencils $S(x)$ satisfy some geometric properties depending on the local geodesic potential $\mathcal{P}(x, \cdot)$. An adaptive construction of such stencils was introduced in [8], which led to breakthrough improvements in terms of computation time and accuracy for strongly anisotropic geodesic energy potentials, as in our application. It invokes Lattice Basis Reduction, a tool from discrete geometry which combines in an optimal way the geometric structure given by the Riemannian metric, and the arithmetic structure of the cartesian discretization grid.

2.3. Curve Length calculation and Geodesic Extraction

The minimal path γ_x of (2) is generically unique, and its euclidean length $\mathcal{V}(x)$ is a crucial ingredient of our algorithm. An approximation of $\mathcal{V}$ is given by the solution of the following fixed point problem: find $V : Z \to \mathbb{R}$ such that (i) for all keypoints $x \in \mathcal{K}$, $V(x) = 0$, and (ii) for all $x \in Z \setminus \mathcal{K}$, denoting by y_x the point at which the minimum (6) is attained

$$V(x) = \|y_x - x\| + \mathrm{I}_{S(x)} V(y_x).$$

A single pass solve is again possible: whenever the Fast Marching algorithm updates $U(x)$, simultaneously update $V(x)$, using the (just computed) minimizer from (6). The minimal path γ_x itself is extracted by following the direction field $(y_x - x)_{x \in Z}$.

3. PATH SCORE BASED KEYPOINTS SEARCHING

Our vessel tree extraction method is embedded within the inner loop of the fast marching algorithm, which it augments with several robust criteria for keypoint selection (tree nodes), adaptation of a path score threshold, and termination.

The approximate geodesic distance $U(x)$ to the currently extracted tree structure is estimated using the classical fast marching algorithm: initialization and steps 1-9 of the loop in the table of Algorithm 1. Following the dynamic programming principle, image pixels are tagged as *Trial* or *Accepted*. The *Trial* point x currently minimizing U is tagged *Accepted* (i.e. frozen), and the value $U(y)$ at neighboring points y is suitably updated. In addition, line 7, we estimate the geodesic curve length $V(y)$, and potentially tag y as *Trial* - an "unfreezing" procedure needed because some new source points, the tree nodes, are introduced as the loop executes.

The original KPSM [3] adds the currently active point x to the set $\mathcal{K}$ of keypoints as soon as $V(x) \geq \lambda$, where λ is the user chosen CLT. This operation, which amounts to lines 15, 16, 18, 19 of our algorithm, yields a tree with branches of length exactly λ. Our algorithm in contrasts extracts vessel tree branches of length within $[\lambda, 3\lambda[$, selected based on a *path score*, see line 17 and (7) below. As a result, it can reliably handle a much smaller CLT λ than the inspirational [3], without leaking outside of the vessel structure, but staying right in its centerline. One or several path score thresholds $T_1 \geq \cdots \geq T_k$ are given as input; generally $k \in \{1, 2\}$, and by convention $T_0 = +\infty$. If the currently active point x has an excessive estimated curve length $V(x) \geq 3\lambda$, see line 10, then the next threshold T_{i+1} is activated in order to discover finer, less visible vessel structures; unless $i = k$ in which case the method ends.

If the currently active point x has an appropriate estimated curve length $\lambda \leq V(x) < 3\lambda$, then it is considered as a candidate new keypoint (i.e. a potential node of the vessel tree structure), see line 15. We extract the geodesic γ linking x to the already extracted tree structure, and evaluate its relevance using a path score: defining $\delta_T(h)$ as 1 if $h \leq T$ and 0 otherwise

$$\mathcal{PS}_T(x) = \int_{\widetilde{\gamma}} \hbar\, \delta_T(\hbar) ds \Big/ \int_{\widetilde{\gamma}} \delta_T(\hbar) ds. \qquad (7)$$

In other words the *path score* is the average value of the OOFCM (4) centreline map $\hbar$ along the physical path $\widetilde{\gamma}$, obtained by stripping γ of its abstract radius dimension. The selection test line 17 requires the path score to exceed the current selection threshold T_i. The selector δ_T appearing in (7) is applied with $T := T_{i-1}$ so as to push the keypoint selection towards finer and less visible structures, when $i > 1$, and leave the vicinity of the tree extracted with the previous threshold T_{i-1}.

Algorithm 1 *Vessel Tree Extraction* (in 2D+radii case)

Input: Metric $\mathcal{M}$, startpoint $\mathbf{p}_s$, curve length threshold λ , *path score* thresholds $(T_i)_{1 \leq i \leq k}$, centerline map $\hbar$.
Output: Paths Γ, keypoint set $\mathcal{K}$.
Initialization:
For each point x, set $U(x)$=$V(x)$=$+\infty$; Tag x as *Trial*.
Set $U(\mathbf{p}_s)$=$V(\mathbf{p}_s)$=0, $\mathcal{K} \leftarrow \{\mathbf{p}_s\}$ and $\Gamma \leftarrow \{\mathbf{p}_s\}$. Set $i \leftarrow 1$.
Marching Loop:
1: Find x, the *Trial* point which minimizes U.
2: Tag x as *Accepted*. ▷ "Standard" fast marching.
3: **for** All y such that $x \in S(y)$ and $U(y) > U(x)$ **do**
4: Compute $U_{\text{new}}(y)$ using (6).
5: **if** $U_{\text{new}}(y) < U(y)$ **then**
6: Set $U(y) \leftarrow U_{\text{new}}(y)$
7: Update $V(y)$, tag y as trial.
8: **end if**
9: **end for**
10: **if** $V(x) \geq 3\lambda$ **then** ▷ Path score threshold reduction.
11: **if** $i = k$ **then** EXIT **else** $i \leftarrow i + 1$ **end if**
12: **for all** points y on the paths Γ **do**
13: Set $U(y) = V(y) = 0$, tag y as *Trial*.
14: **end for**
15: **else if** $V(x) \geq \lambda$ **then** ▷ Keypoint selection.
16: Track the minimal path γ from x.
17: **if** $\min\{\mathcal{PS}_{T_{i-1}}(x), \hbar(x)\} \geq T_i$ **then**
18: Append x to keypoints $\mathcal{K}$, and γ to edges Γ.
19: Set $U(x) = V(x) = 0$, tag x as *Trial*.
20: **end if**
21: **end if**

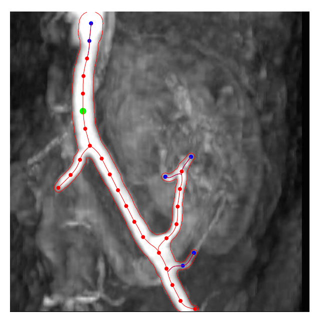

Fig. 1. Demonstration of the proposed method (see text).

4. EXPERIMENTS

The proposed method requires several parameters, as described in Algorithm 1. Specifically, the Curve Length Threshold (CLT) λ should be slightly more than twice the largest radius of the vessels to be detected. The path score thresholds $(T_i)_{i=1}^k$, with $k \in \{1, 2\}$ depending on the test case, are automatically selected as quantiles of the OOFCM (4) distribution on image pixels. The user given starting

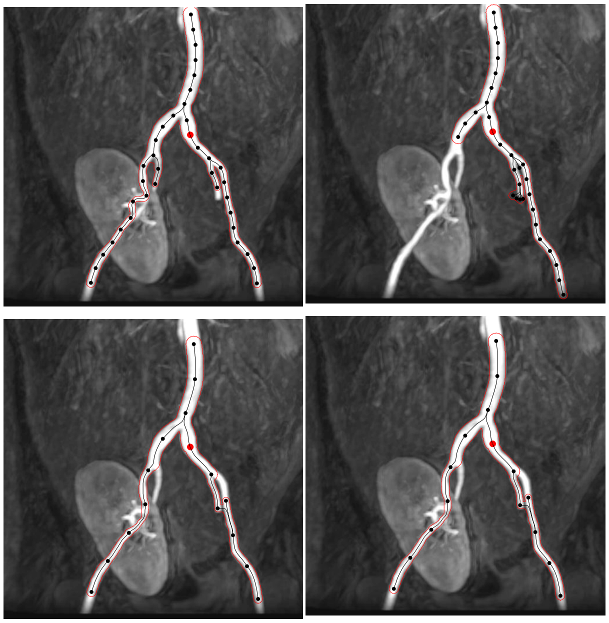

Fig. 2. Segmentation results of our method (left) and the classical KPSM (right), with a small (top) or large (bottom) curve length threshold.

keypoint is colored in red or green and supersized, while keypoints obtained with the second threshold are shown blue.

4.1. Advantages of using a small CLT and a *path score*

Small curve length thresholds (CLT) are a-priori desirable when extracting vessel trees, since they favor the discovery of small structures and avoid the extraction of inadequate shortcuts linking different tree branches. Unfortunately, the classical keypoints selection [3] suffers from a leaking problem with small CLT: before the main vessel branches are extracted, multiple irrelevant keypoints are detected outside the vessel structure of interest. This problem, which is mainly caused by noise and intensity inhomogeneities, is avoided with our new keypoint selection criterion involving a *path score*, as illustrated on Figure 2.

On the *bottom* of Figure 2, with a large CLT $\lambda = 60$, the two methods produce similarly inaccurate results: some small branches are missed, and some undesirable shortcuts between different branches are extracted. On *top* of Figure 2, with a small CLT $\lambda = 26$, the KPSM [3] keypoints leak and begin to accumulate outside the structure (right); in contrast our method accurately detects the vessel tree and then automatically stops (left).

4.2. Experimental results in a complex vessel network

We illustrate on Figure 3 the results of our method, with CLT $\lambda = 12$, and the classical KPSM [3] with CLT $\lambda = 50$, which

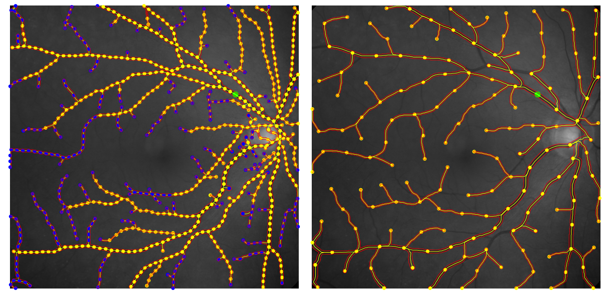

(a) (b)

Fig. 3. Results of our method (a) and classical KPSM (b): red point is the startpoint and yellow points are keypoints.

empirically are the best for these two methods on this image. As discussed in section 4.1, many vessels are missed with a large CLT, are numerous irrelevant shortcuts are extracted.

The impact of the second curve length threshold T_2 is illustrated on Figure 4. The smaller threshold T_2 used in (b) allows to detect more vessels, but meanwhile some non-vessels paths are also collected.

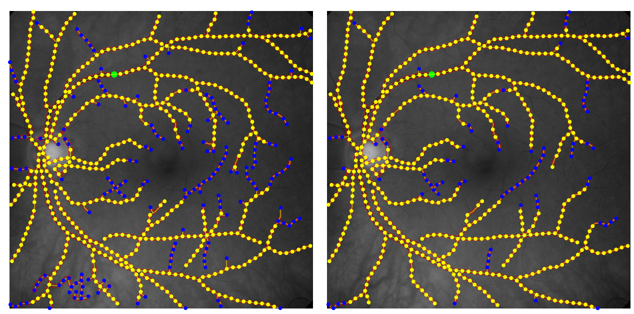

(a) (b)

Fig. 4. Results of our method with a small (a) or large (b) second threshold T_2. Start point in green, keypoints extracted with first threshold T_1 in yellow, and with second threshold T_2 in blue.

5. CONCLUSIONS

In this paper, we propose a new keypoint based vessel tree extraction method using Anisotropic Fast Marching, and introducing of a *path score* in the keypoint selection criterion. These ingredients allow our method to search keypoints separated by small curve lengths, leading better extraction results compared to the classical keypoints searching method. Numerical experiments illustrate these improvements on two retinal images and two MRA images. The next step is to extend our approach to 3D and to validate it on a large data set.

6. REFERENCES

[1] G. Peyré, M. Péchaud, R. Keriven, and L. D. Cohen, "Geodesic Methods in Computer Vision and Graphics, Foundations and Trends in Computer Graphics and Vision," pp. 197–397, 2010.

[2] F. Benmansour and L. D. Cohen, "Tubular Structure Segmentation Based on Minimal Path Method and Anisotropic Enhancement," *International Journal of Computer Vision*, vol. 92, no. 2, pp. 192–210, 2011.

[3] F. Benmansour and L. D. Cohen, "Fast object segmentation by growing minimal paths from a single point on 2D or 3D images," *Journal of Mathematical Imaging and Vision*, vol. 33, no. 2, pp. 209–221, 2009.

[4] L. D. Cohen and R. Kimmel, "Global minimum for active contour models: A minimal path approach," *International Journal of Computer Vision*, vol. 24, no. 1, pp. 57–78, 1997.

[5] H. Li and A. Yezzi, "Vessels as 4-D curves: Global minimal 4-D paths to extract 3-D tubular surfaces and centerlines," *IEEE Transactions on Medical Imaging*, vol. 26, no. 9, pp. 1213–1223, 2007.

[6] J. N. Tsitsiklis, "Efficient algorithms for globally optimal trajectories," *IEEE Transactions on Automatic Control*, vol. 40, no. 9, pp. 1528–1538, 1995.

[7] J. A. Sethian, "Fast marching methods," *SIAM Review*, vol. 41, no. 2, pp. 199–235, 1999.

[8] Jean-Marie Mirebeau, "Anisotropic Fast-Marching on cartesian grids using Lattice Basis Reduction," *to appear, preprint available on Arxiv*.

[9] Qingfen Lin, "Enhancement, Extraction, and Visualization of 3D volume data," *Ph.D. Thesis, Linkoping University*, 2003.

[10] V. Kaul, A. Yezzi, and Yichang Tsai, "Detecting curves with unknown endpoints and arbitrary topology using minimal paths," *IEEE Transactions on PAMI*, vol. 34, no. 10, pp. 1952–1965, 2012.

[11] T. Deschamps and L. D. Cohen, "Fast extraction of minimal paths in 3D images and applications to virtual endoscopy," *Medical Image Analysis*, vol. 5, no. 4, pp. 281–299, 2001.

[12] H. Li, A. J. Yezzi, and L. D. Cohen, "3D multi-branch tubular surface and centerline extraction with 4D iterative key points," *In MICCAI*, pp. 1042–1050, 2009.

[13] Liao Wei, Wörz Stefan, and Rohr Karl, "Globally Minimal Path Method Using Dynamic Speed Functions Based on Progressive Wave Propagation," *in ACCV*, pp. 25–37, 2012.

[14] Max W. K. Law and Albert C. S. Chung, "Three Dimensional Curvilinear Structure Detection Using Optimally Oriented Flux," *In ECCV 2008*, pp. 368–382, 2008.